Shear wave attenuation measurements from converted-wave VSP data

Michelle C. Montano, Don C. Lawton, and Gary F. Margrave

ABSTRACT

Q_S values were estimated from converted-wave VSP data using the spectral-matching method. These values were computed from a walk-away VSP. Then, we conveyed these results into a single value at zero-offset by using the QVO method. For this study, Q_S values determined range from 20 to 50, suggesting a strong attenuation for the shear waves. Moreover, we were able to compare Q_S/Q_P ratios versus V_P/V_S ratios to understand the rock properties of the study area.

INTRODUCTION

Shear wave attenuation can be measured from down-going shear waves in VSP (Montano et al., 2014). However, direct shear waves are not always easy to identify. One problem associated with these waves is that after a short distance, they lose a significant part of their bandwidth and energy. It is well known that shear waves usually attenuate faster than P-waves (Mavko and Nur, 1979, Winkler and Nur, 1982, Udias, 1999, Montano et al., 2014). Also, it is important to note that direct shear waves have to travel through the near surface. This probably causes a severe attenuation in the downgoing S-wave energy recorded in VSP data (Fig. 1). If we want to estimate reliable Q_S values along the borehole receivers, this may be a problem. An alternative method to estimate Q_S is through exploiting converted-waves (P-S) reflections. In this case, the downward seismic wave-field travels as a P-wave and reflects as an S-wave. As a result, the initial S-waves at the conversion point has the same bandwidth as the incident P-wave. This enables us to obtain more reliable Q_S estimations along the borehole.

For this study, we processed the same field VSP data previously used in Montano et al., 2014. Here, we analysed the shot points 6 to 14 to study converted-waves. Then, we decided to focus our attention to the shot points 6 to 9 (Fig. 2), which are closer to the borehole receiver and also have less noise related to the travel-time distance.

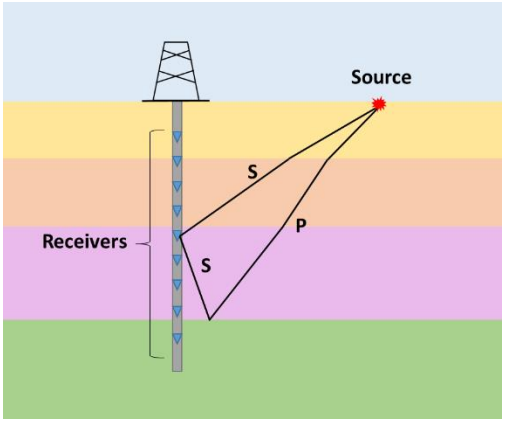

FIG. 1. Down-going shear waves and converted-waves travelling to the borehole receivers.

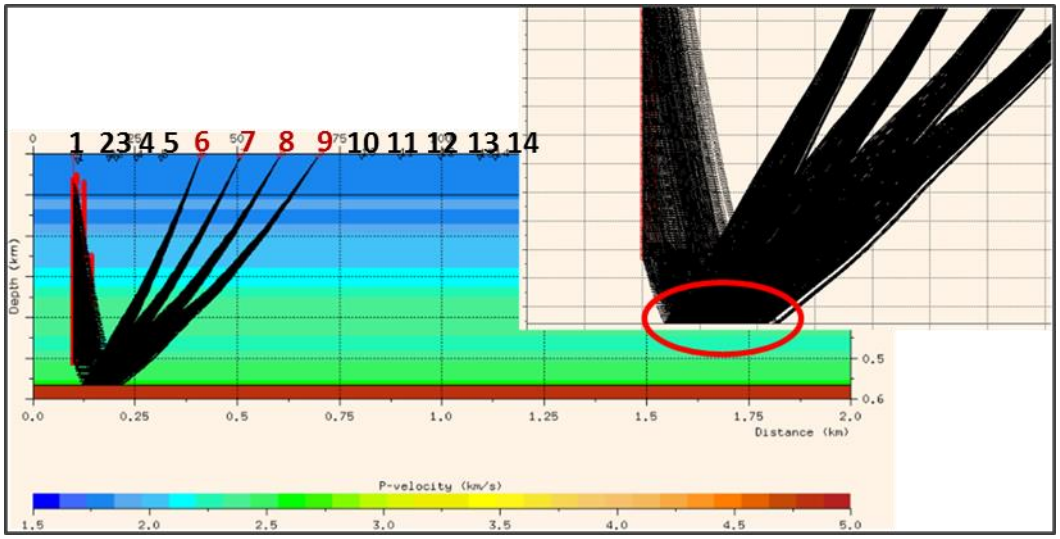

FIG. 2. Ray-tracing for shot points 6 – 9 using NORSAR2D software. P-wave and shear wave velocities were obtained from well logs and calibrated with the VSP data. For this model, velocities in the overburden were set to increase linearly. Shot points and borehole receivers have a true relative distance.

THEORY

Spectral matching method

Qs values were computed using the spectral matching method in Matlab (CREWES software) which is explained in Figure 3. A seismic trace, S_1, at depth Z_1, and a second trace, S_2 at depth Z_2, were selected for a given time window pair, where $Z_2 > Z_1$. Then, a Fourier transform was applied to compute their amplitude spectrum. Q values were estimated by minimizing the difference between amplitude spectra. For more details about this method, the reader is referrer to Margrave, 2013.

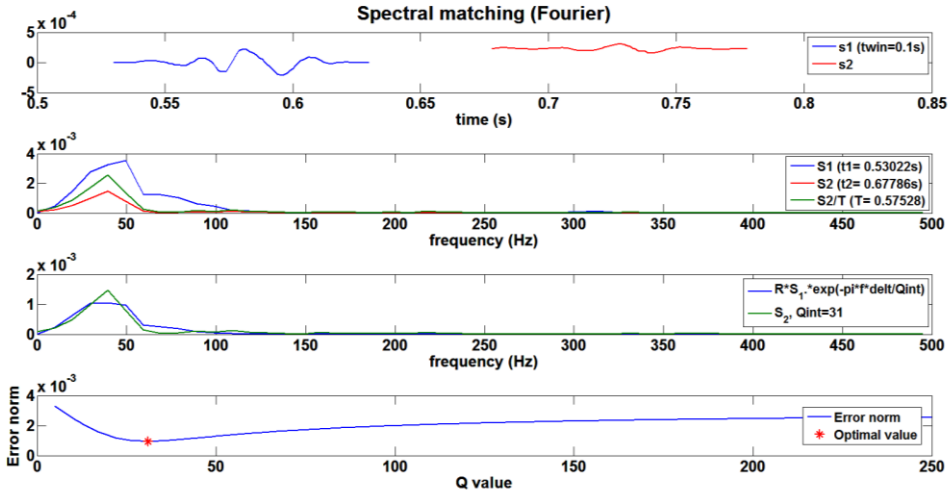

FIG. 3. Q_S estimation from converted-waves using spectral matching (Shot point: 7).

Hodogram rotation

In order to process the converted-waves, we applied two rotations to the seismic gathers (Fig. 4). The first rotation was computed with the horizontal components, X and Y, in which a rotation with an angle β is applied to obtain a maximum horizontal component Hmax or X' (Hinds et al., 1996). In Figure 5, we can observe the results obtained for the shot point 12 after this first rotation. The second rotation was computed using the vertical and horizontal components, Z and Hmax respectively. In this case, Hmax was rotated toward the reflector or incidence point (α angle rotation). Figure 6 shows the results obtained after the second rotation in which we obtained Hmax'.

If we compare Figures 5 and 6, we observe a very subtle difference between these seismic gathers. However, if we compare the vertical component before and after these two rotations (Fig. 7 and 8 respectively), we notice that most of the converted shear wave energy has been removed. This led us to conclude that the hodogram rotation implemented here is robust and most of the up-going S-wave energy is contained on the Hmax' component.

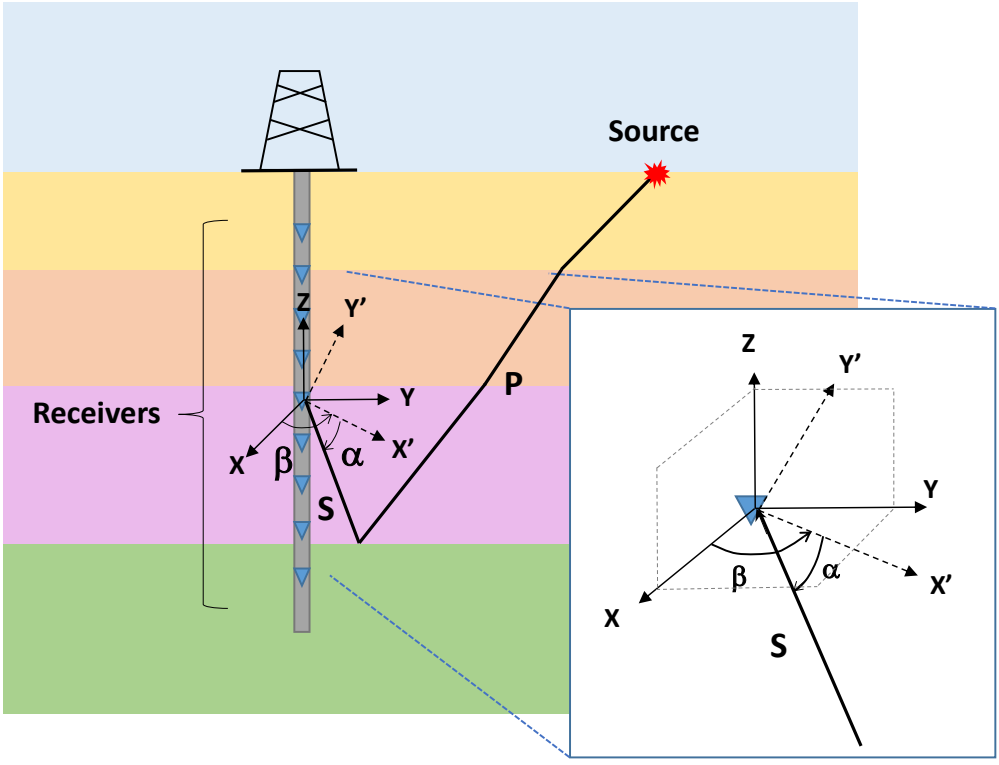

FIG. 4. Sketch showing rotation 1 (horizontal components: β angle rotation) and rotation 2 (vertical and hmax component: α angle rotation).

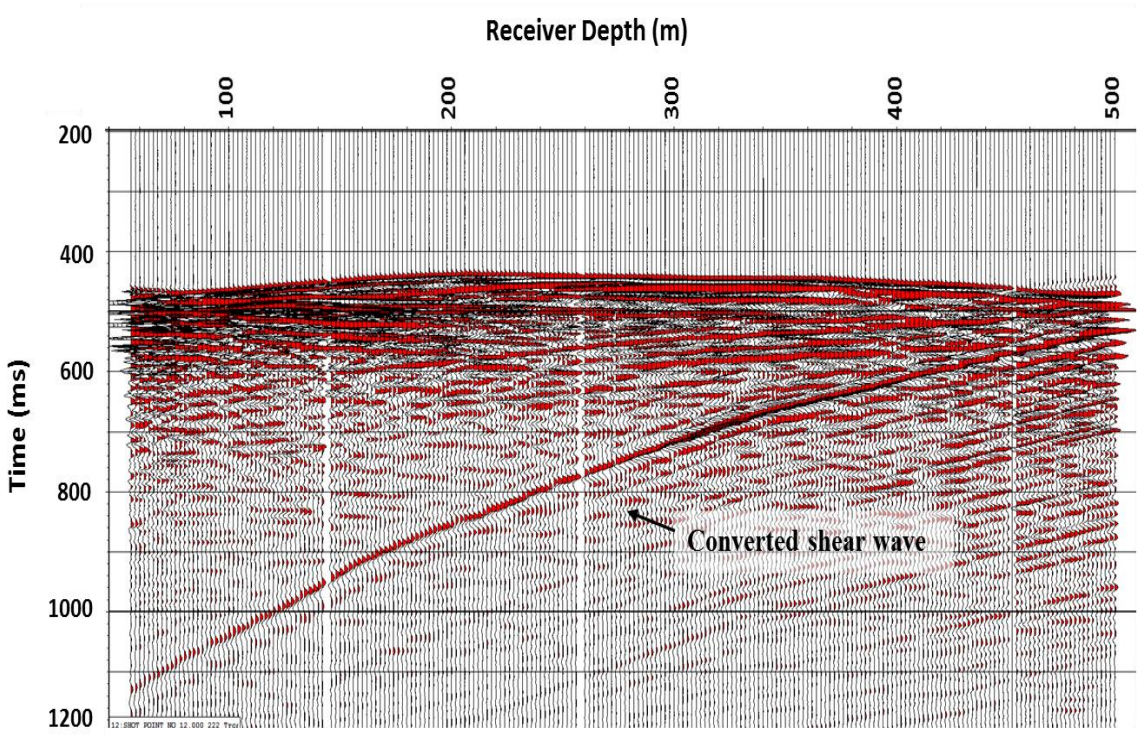

FIG. 5. Seismic gather for shot point 12 after first rotation (Hmax): a β angle rotation was applied to the horizontal components (X and Y).

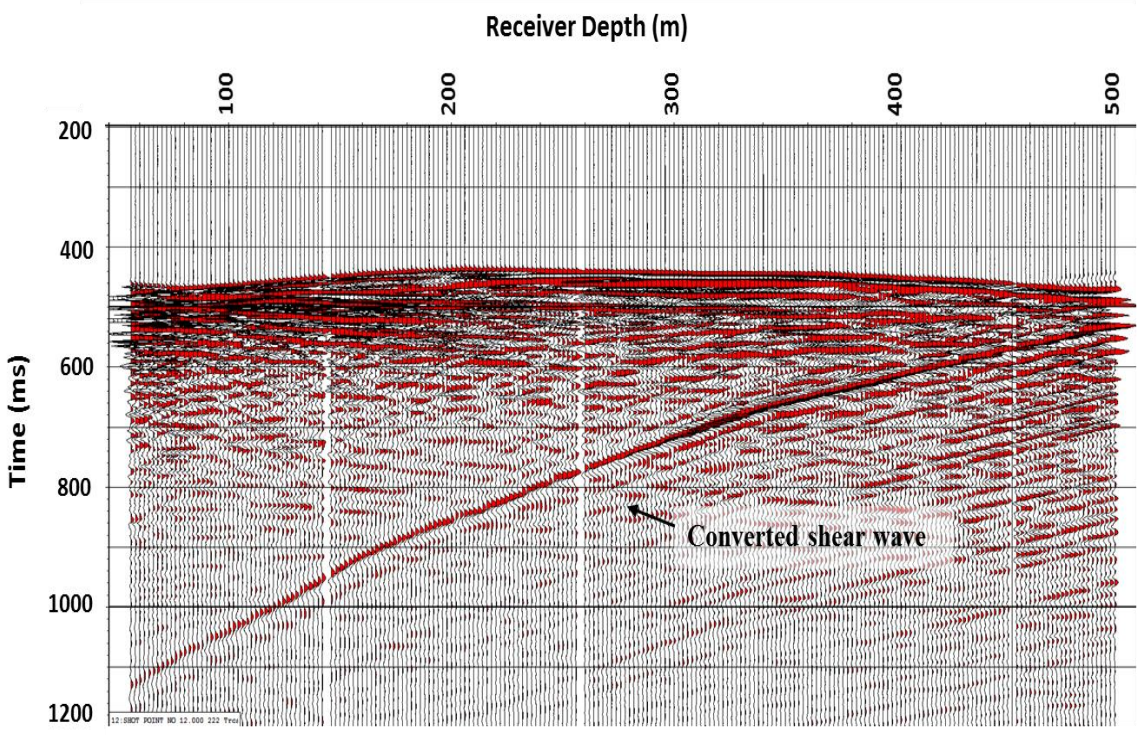

FIG. 6. Seismic gather for shot point 12 after second rotation (Hmax'): an α angle rotation was applied to the vertical and horizontal components (Z and Hmax).

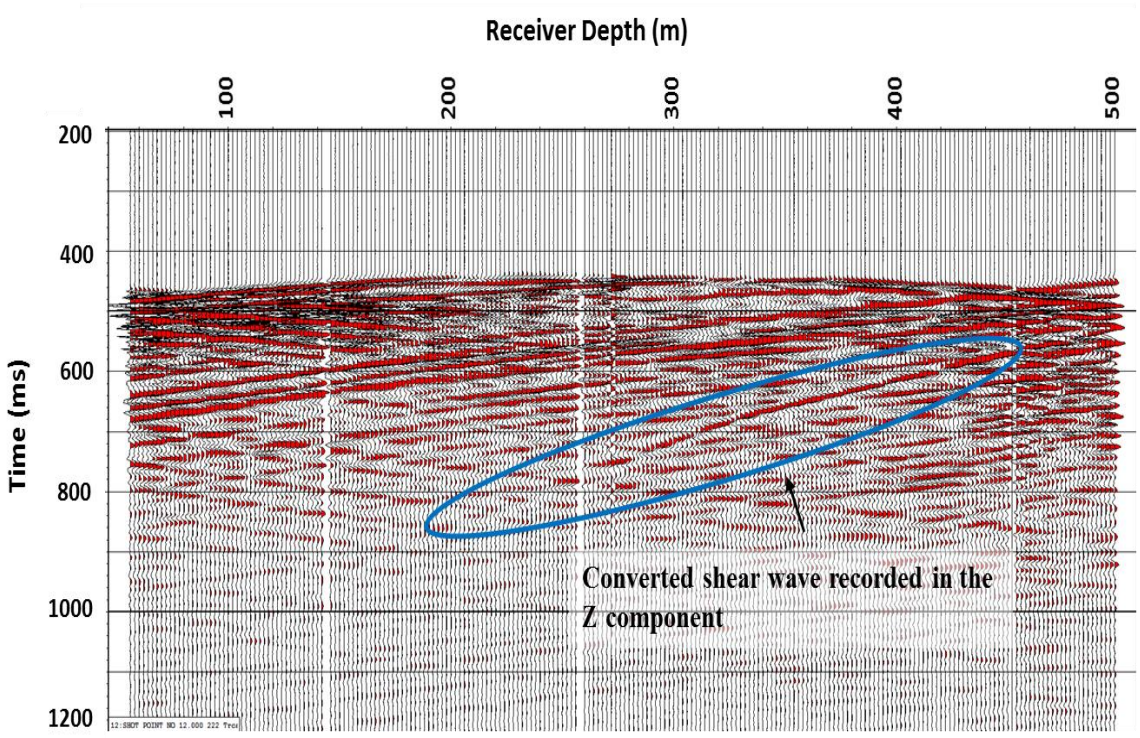

FIG. 7. Seismic gather for shot point 12. Raw vertical component (Z).

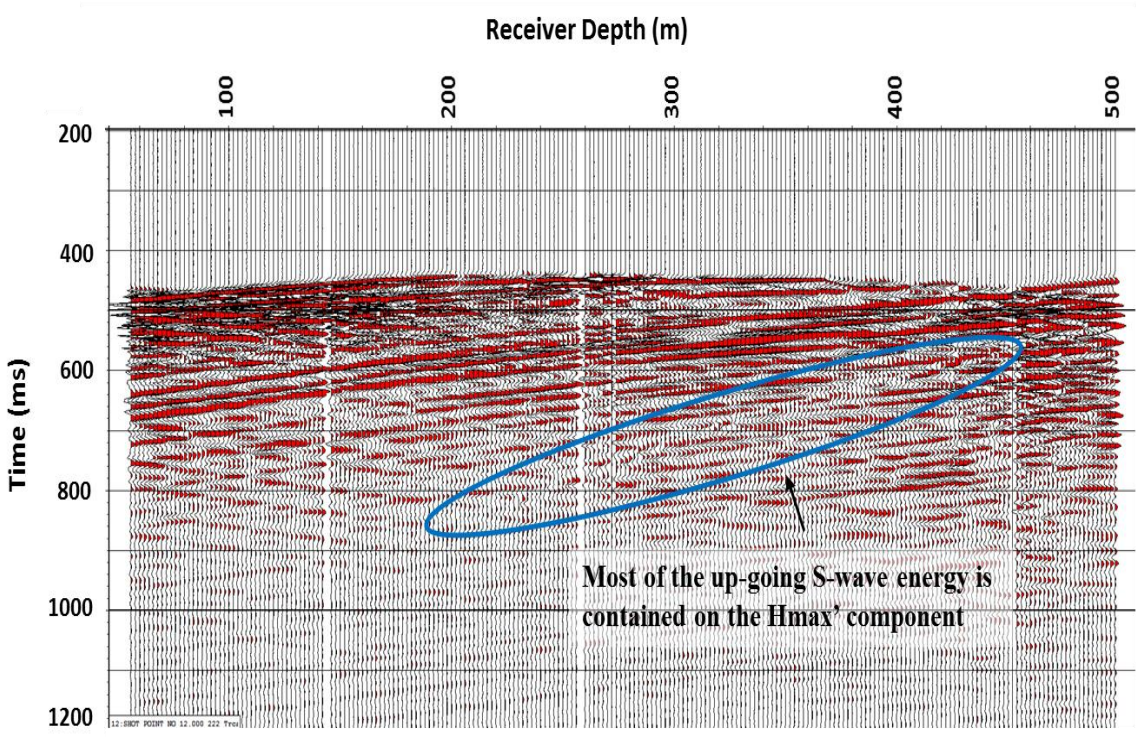

FIG. 8. Seismic gather for shot point 12 – Raw Vertical'. Vertical component (Z) after second rotation.

QVO method

Q vs offset method was first introduced by Dasgupta and Clark (1998), in which Q values were estimated from surface seismic by processing CMP gathers. For this study, they used the spectral ratio method. There, they noticed that spectral ratio slopes change with offset due to different raypath geometries. The key point here is how to convey all these values into one for a given common mid-point. For answering this question, they assumed that Q values change linearly with offset squared because reflected traveltime changes are also dependent on offset squared. Therefore, the Q value for the zero-offset condition can be estimated by computing the intercept of a linear fit over Q versus offset squared values.

Figure 10 shows the QVO method with some variations. For this case, we used converted-waves from VSP data to estimate Q_S. We assumed that converted shear waves show a close to vertical raypath geometry after reflection (Fig. 2). Also, the common conversion points are very close together for different shot points. This led us to state that the converted-waves or up-going shear waves recorded at a given receiver depth share a similar conversion point. Then, for this specific study we were able to use the QVO method for converted-waves in VSP data. This method helped us to convey our Q_S estimation from walk-away data (Fig. 9) to zero-offset data (Fig. 11).

ANALYSIS

Figure 9 shows the Q_S values estimated from the converted-waves for shot point 6 to 9 using the spectral matching method. As one can see, these results show a similar trend in which Q_S values range from 20 to 50. We were expecting this to happen because of the traveltime geometry for the converted-wave. The locations were Q_S is higher than 100, we could not estimate Q due to noise in the data (especially shot points 6 and 9). For this reason, we obtained more reliable results by integrating these four Q_S estimations into one (Fig. 11).

After computing Q_S for each shot point, we estimated Q_S at zero-offset by using the QVO method. Results are shown in Figure 11. There, we observed a strong correlation between Q_S estimation and the formation tops. We also noticed a decrease in Q_S values from 320m to 370m depth. Suggesting that there may exist an additional mechanism causing shear wave attenuation.

Using Q_P values obtained from our previous report (Montano et al., 2014), we were able to compute the Q_P/Q_S ratio (Fig. 12). For this case, we also observed that Q_P/Q_S ratio changes are related to lithology changes. Also, there is a high Q_P/Q_S value between formation top F and G. This may be related to changes in lithology or fluid saturation.

Seismic Attenuation versus velocity

In order to have a better understanding of the relationship between seismic attenuation and rock properties, we compared seismic attenuation versus velocities (Fig. 13). According to Mavko and Nur (1979) and Winkler and Nur (1982), P-wave attenuation in partially saturated rocks is much stronger than shear wave attenuation. However, in fully saturated rocks shear wave attenuation is stronger than P-wave attenuation. The value

$Q_S/Q_P=1$ can be used as a reference to separate partial saturation ($Q_S/Q_P>1$) from total saturation ($Q_S/Q_P<1$) (Figure 17 in Winkler and Nur, 1982).

In Figure 13, velocities were obtained from well logs after a moving average filter was applied to match the resolution of the logs with the resolution of the attenuation estimations. For this study, water saturation logs were not available. For this reason, we coloured the scatter-plots by gamma-ray and depth. This may help us to have a general idea of fluid saturations along the borehole. Following the previous analysis, the blue circle in Figure 13 we interpret to represent partially saturated rocks and the red circle represents fully saturated rocks. Notice that points enclosed by the red circle show high gamma-ray values. This may indicate shaly sediments, in which high water saturation is usually found. Also, we can observe in the scatter-plot coloured by depth that the blue box enclose points located over 400m depth which is close to the transition zone. This suggests that partially saturated rocks are present in this area.

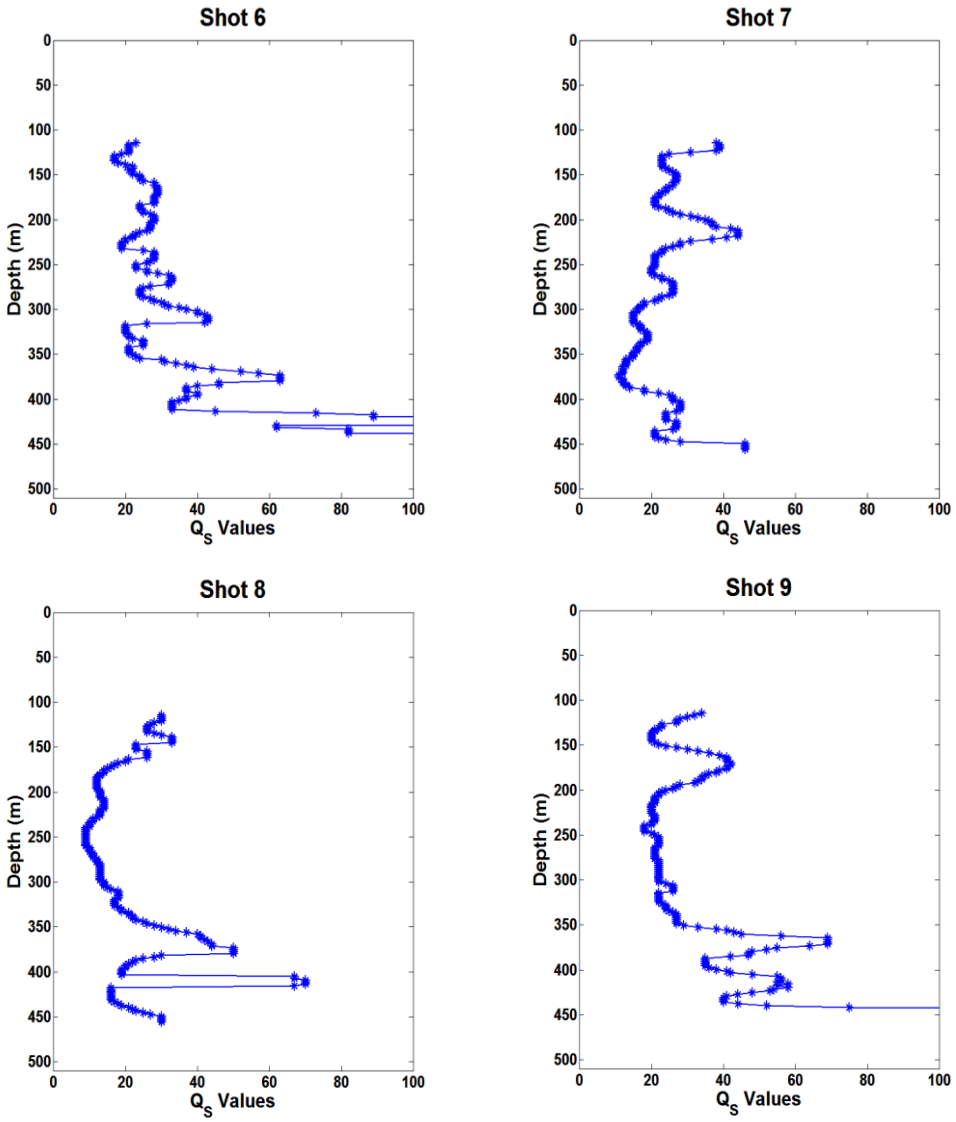

FIG. 9. Q_S estimation from converted-wave data using spectral matching method.

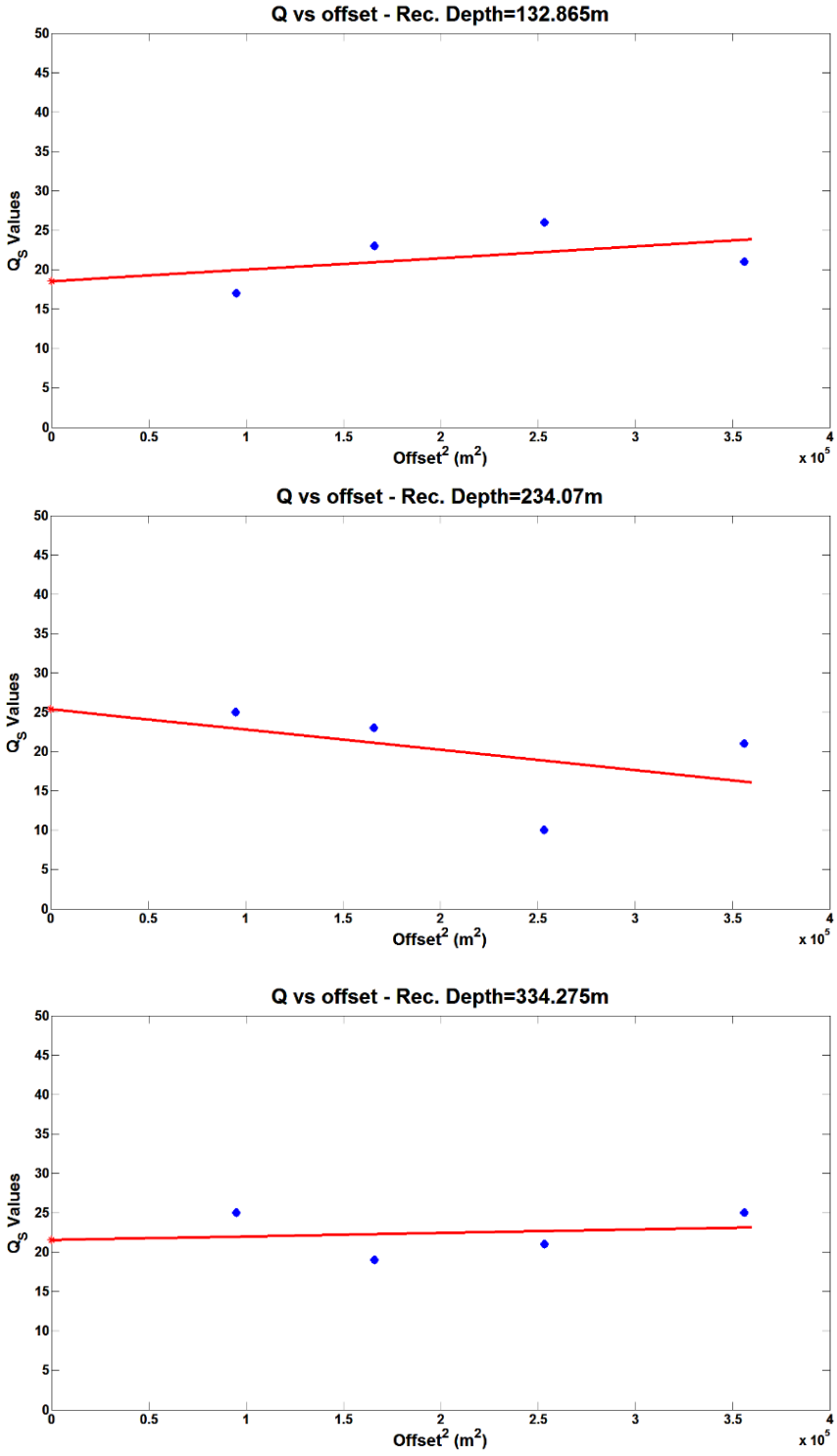

FIG. 10. Crossplot: Q versus offset^2 for receiver depths = 132m, 234m and 334m.

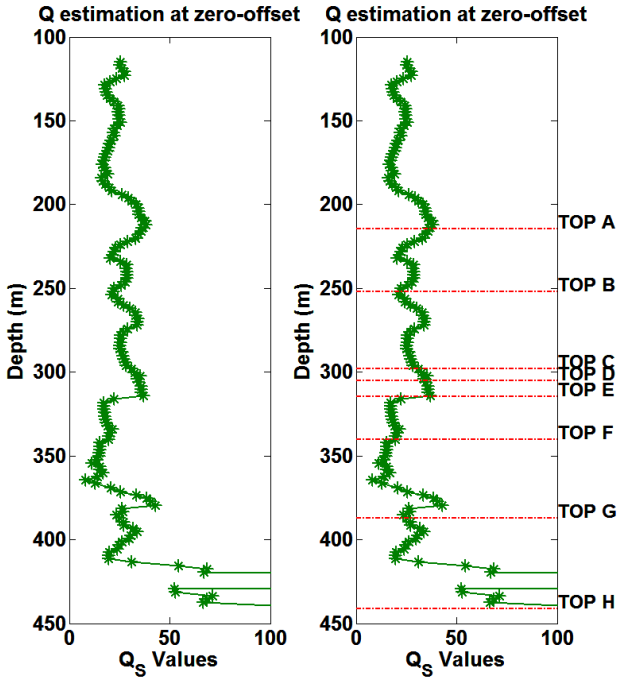

FIG. 11. Left: Q_S estimation at zero-offset using QVO method and right: including formation tops.

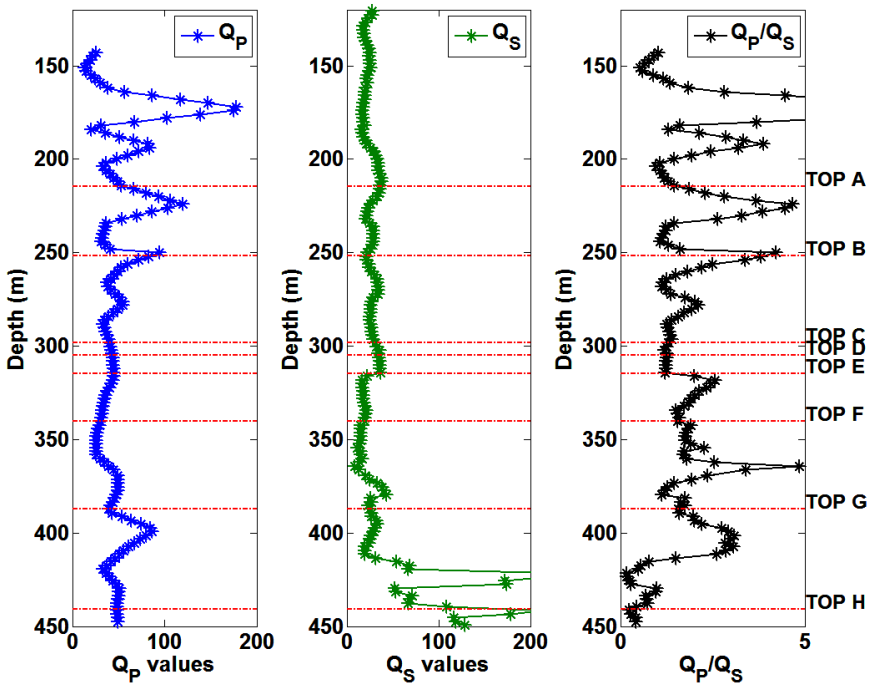

FIG 12. Q_P values from previous report (Montano et al., 2014), Q_S values from converted-waves and Q_P/Q_S estimation.

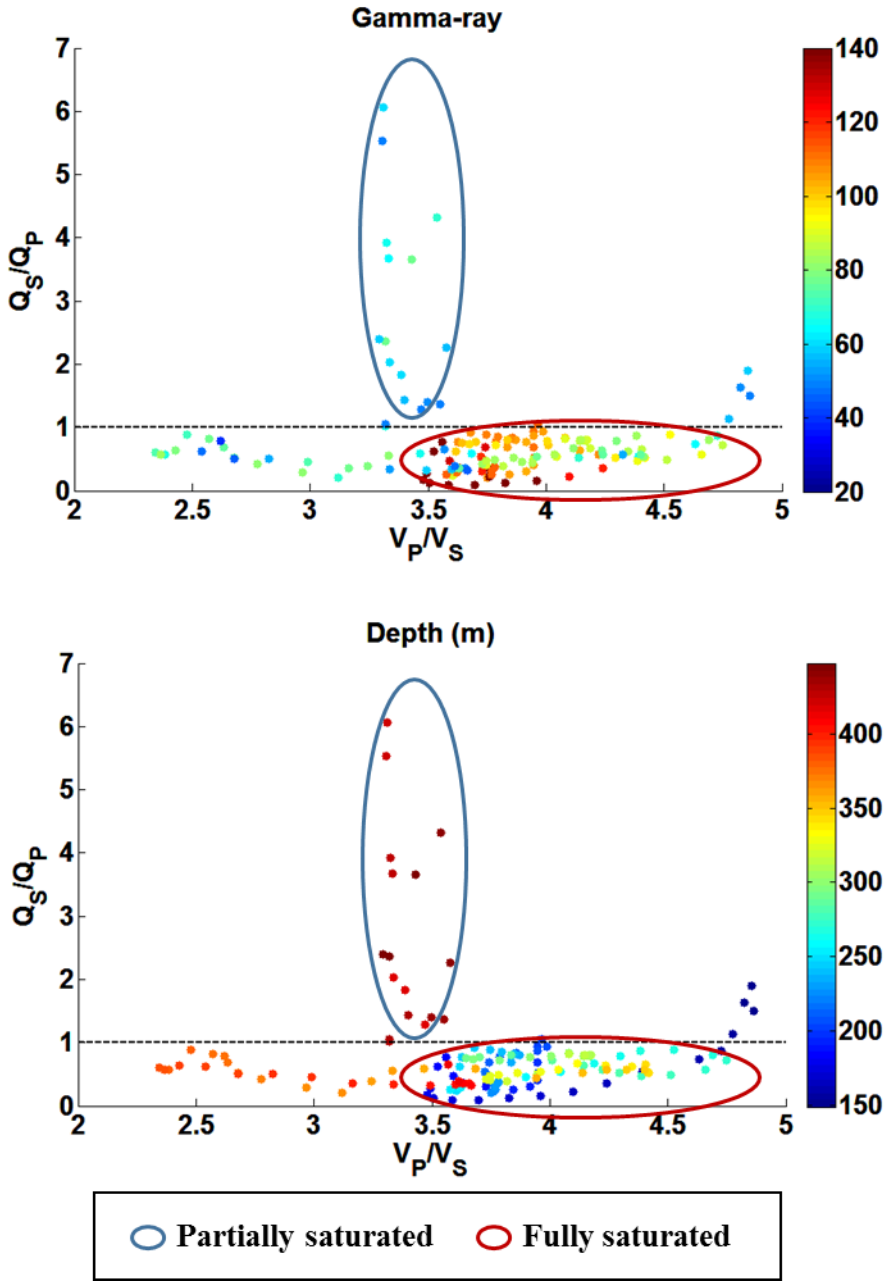

FIG. 13. Seismic attenuation ratio versus velocity ratio scatter-plot. Top: Q_S/Q_P versus V_P/V_S coloured by gamma-ray and, bottom: coloured by receiver depth (m).

CONCLUSIONS

Converted-wave data may help us to obtain more reliable Q_S estimation. These waves are more complex but we can use their unique characteristics in our favor in order to estimate Q values, particularly for up-going wave-fields.

Using hodogram rotation for converted-wave VSP data is a good alternative, particularly when we do not count with an accurate velocity model that includes the overburden to compute the ray-tracing. Hodogram analysis is usually applied to rotate one component in VSP data. However, results show that this method can be also used to focus the energy of the converted-waves.

The QVO method which is usually used for surface seismic data helped us to convey our Q_S estimations from VSP converted-wave data. Q_S values range from 20 to 50 approximately.

In order to do a comprehensive reservoir characterization, it is necessary to understand the rock properties of the area. Seismic attenuation may help us to be one step closer to this goal. Results show that we can compare seismic attenuation versus velocities to identify fluid saturation changes in rocks.

FUTURE WORK

Further study about the relationship between seismic attenuation and rock properties is needed. These values can be used to estimate gas saturation and lithology discrimination, among other properties.

We will estimate Q in a deeper data set with more layers and noise. For this case, we will need to apply a stronger filter to remove noise and separate the wave-field. The challenge will be to pre-process the data set without changing the amplitudes. Then, we will be able to obtain some reliable Q estimation by applying the same methods.

ACKNOWLEDGEMENTS

The authors thank the sponsors of CREWES for continued support. This work was funded by CREWES industrial sponsors and NSERC (Natural Science and Engineering Research Council of Canada) through the grant CRDPJ 461179-13. Michelle Montano was also supported by a 2014/2015 scholarship from the CSEG Foundation. We also thank an unidentified company for access to the field VSP data, GEDCO/Schlumberger for providing the VISTA software and NORSAR for providing the NORSAR-2D software.

REFERENCES

Dasgupta R. and Clark R. A., 1998. Estimation of Q from surface seismic reflection data. GEOPHYSICS, 63(6), 2120-2128. doi: 10.1190/1.1444505

Hinds, R. C., Anderson, N. L., and Kuzmiski, R. D., 1996, VSP Interpretive Processing: Theory and Practice, Soc. Expl. Geophys.

Margrave, G. F., 2013, Q tools: Summary of CREWES software for Q modelling and analysis: CREWES Research Report, 25, 56.1-56.22.

Mavko G. M. and Nur A., 1979. Wave attenuation in partially saturated rocks. GEOPHYSICS, 44, 161-178. doi: 10.1190/1.1440958

Montano, M. C., Lawton, D. C., and Margrave, G. F., 2014. Shallow Q_P and Q_S estimation from multicomponent VSP data: CREWES Research Report, 26, 55.1-55.24.

Udias, A., 1999, Principles of Seismology, Cambridge University Press.

Winkler K. W. and Nur A., 1982. Seismic attenuation: Effects of pore fluids and frictional sliding. GEOPHYSICS, 47(1), 1-15. doi: 10.1190/1.1441276